Supporting Information

A Nanosystem of Amphiphilic Oligopeptide-Drug Conjugate Actualizing Both αvβ3 Targeting and Reduction-Triggered Release for Maytansinoid

Yanqin Liang[1,2,*], Suxin Li[2,*], Xiaoyou Wang[2], Bo He[2], Bing He[2], Wenbing Dai[2], Hua Zhang[2], Xueqing Wang[2], Yiguang Wang[1,2], Demin Zhou[1], Qiang Zhang[1,2,✉]

1. State Key Laboratory of Natural and Biomimetic Drugs, School of Pharmaceutical Sciences, Peking University, Beijing 100191, China
2. Beijing Key Laboratory of Molecular Pharmaceutics, School of Pharmaceutical Sciences, Peking University, Beijing 100191, China

* Both authors contributed equally to this manuscript.

✉ Corresponding author: Qiang Zhang, Telephone: +86 10 82802791, Fax: +86 10 82802791, E-mail address: zqdodo@bjmu.edu.cn

Table of Content

1. Supplementary Methods and Measurements

1.1 Materials……3

1.2 Synthesis and Characterization of Amphiphilic Peptide-DM1 Small Molecule Conjugates (APDCs) ……3

1.3 Interaction between Various APDC@NPs and Integrin αvβ3 Detected by Surface Plasmon Resonance (SPR) Technology……8

1.4 Cell culture……8

1.5 Preparation and Characterization of Various Cy3.5-loaded APDC@NPs……8

1.6 Immunofluorescence for Integrin αvβ3 Expression……9

1.7 Animals……10

1.8 TUNEL Analysis……10

1.9 Immunohistochemical Analysis……11

2. References……11-12

3. Table……13

4. Figures……14-43

1. Supplementary Methods and Measurements

1.1 Materials

Maytansinoid DM1 was purchased from Borui Pharmaceutical (Suzhou) Co., Ltd. (Suzhou, China). Cyclic (Arg-Gly-Asp-d-Phe-Lys) (cRGDfK) peptide (molecular weight = 603.8500) and Cyclic (Arg-Pro-Gln-d-Phe-Lys) (cRPQfK) peptide (molecular weight = 656.82) were purchased from GL Biochem (Shanghai) Ltd. (Shanghai, China), these two peptides are cyclic structure, including five amino acid number, and soluble in water. Cy3.5 NHS ester was obtained from Lumiprobe company. Dithiothreitol (DTT) was purchased from Merck Company (Germany) and glutathione ethyl ester (GSH-OEt) was purchased from Adipogen (Korea). CM-5 sensor chips were obtained from GE Healthcare Bio-Sciences AB (Uppsala, Sweden). Dynasore, Cytochalasin D, the antibody of CD31 and Ki67 were obtained from Abcam (Cambridge, UK). Hoechst 33258 was obtained from Molecular Probes Inc. (Eugene, USA). Sulforhodamine B (SRB) and Tris base were obtained from Sigma-Aldrich (St. Louis, MO, USA). Cell cycle detection kit and tumor immunohistochemical detection kit were supplied by Beyotime Biotechnology (Shanghai, China). RPMI-1640 with L-glutamine medium, Ham's F12K-Medium, penicillin-streptomycin liquid (100×) and 0.25% trypsin were purchased from M&C Gene Technology (Beijing, China). Fetal bovine serum was purchased from GIBCO, Invitrogen Corp. (Carlsbad, CA, USA). All other solvents and reagents were analytical grade and used as received.

1.2 Synthesis and Characterization of Amphiphilic Peptide-DM1 Small Molecule Conjugates (APDCs)

In our study, all amphiphilic peptide-maytansinoid DM1 small molecule conjugates were synthesized as illustrated in Figure S1-S4. In order to generate the

thioether-linked peptide-maytansinoid DM1 conjugates, the maytansinoid DM1 was modified with succinimidyl-4-(*N*-maleimidomethyl)cyclohexane-l-carboxylate to introduce succinimidyl groups according to reference with some modifications [1]. In brief, the maytansinoid DM1 (165.38 mg, 0.224 mmol) was mixed with the succinimidyl-4-(*N*-maleimidomethyl)cyclohexane-l-carboxylate (50.00 mg, 0.150 mmol) solution in 0.1 M potassium phosphate buffer, pH 6.0. The course of the reaction was followed by thin-layer chromatography (TLC). After completion of the reaction, the conjugate was purified by a silica gel column using dichloromethane/methanol (CH_2Cl_2:CH_3OH, 10:1 v/v) as the eluent to give a white solid (DM1-SMCC). Electrospray ionization mass spectrometry (ESI-MS) m/z $[M+Na]^+$: 1071.3815 (calculated 1071.4530).

The synthesis of cRGD-SMCC-DM1 (RCCD) or cRPQ-SMCC-DM1 (QCCD) conjugate followed the method in reference with some modifications [2]. Briefly, cRGDfK (59.16 mg, 0.098 mmol) or cRPQfK (64.37 mg, 0.098 mmol) was dissolved in anhydrous DMF (1.5 mL), and the pH of the solution was adjusted to 8.0-8.5 with *N*-methylmorpholine at 0 ^oC. After 5 min, the mixture was added to a solution of DM1-SMCC 100.00 mg, 0.093 mmol) and anhydrous DMF (1.5 mL), and the resulting solution was stirred for 24 h under argon dark at room temperature. Then the reaction mixture was precipitated in cold anhydrous ethyl ether. The crude product was purified by a silica gel column using dichloromethane/methanol (CH_2Cl_2:CH_3OH, 10:1 v/v) as the eluent. The product was collected and the solvent was removed by rotary evaporation to give a white solid (89 mg, 61%). ESI-MS m/z $[M+H]^+$ of RCCD conjugate: 1560.7964 (calculated 1561.0130), ESI-MS m/z $[M+H]^+$ of QCCD conjugate: 1614.2056 (calculated 1614.2730) (Figure S7).

In order to generate the disulfide-linked peptide-maytansinoid conjugates, the

cyclic peptides were modified with 2-Pyridyl-2-carboxyethyl Disulfide (Py-SS-MPA) to introduce dithiopyridyl groups. In brief, the cRGD-SS-DM1 (RSSD) or cRPQ-SS-DM1 (QSSD) conjugate was obtained with a three-step method. First, Py-SS-MPA was synthesized and purified on the basis of our previous paper [3]. Second, the synthesis of Py-SS-cRGD or Py-SS-cRPQ, to a solution of Py-SS-MPA (30.78 mg, 0.143 mmol) in anhydrous DMF (0.5 mL), HBTU (108.5 mg, 0.286 mmol) was added to activate the carboxyl of Py-SS-MPA. After 30 min, the solution of cRGDfK (103.44 mg, 0.171 mmol) or cRPQfK (112.31 mg, 0.171 mmol) in anhydrous DMF (1.0 mL) was added to the reaction mixture. Then the pH of the reaction solution was adjusted to 9.0-9.5 with *N*,*N*-Diisopropylethylamine (DIEA), and the reaction mixture was stirred under nitrogen atmosphere for 24 h at room temperature. After completion of the reaction, cold anhydrous diethyl ether was added to produce a light yellow slightly sticky precipitate. The crude product was purified by washing with methanol and collected by filtration to give a light yellow solid (57 mg, 50%). ESI-MS m/z $[M+H]^+$ of Py-SS-cRGD: 801.3196 (calculated 801.5600), ESI-MS m/z $[M+H]^+$ of Py-SS-cRPQ: 853.8794 (calculated 853.8000).

Finally, the synthesis of cRGD-SS-DM1 or cRPQ-SS-DM1 conjugate. Briefly, Py-SS-cRGD (42.2 mg, 0.0527 mmol) or Py-SS-cRPQ (45.0 mg, 0.0527 mmol) was dissolved in DMF (2.0 mL), and then DM1 (46.7 mg, 0.0633 mmol) was added dropwise. The reaction was stirred under nitrogen atmosphere dark at room temperature for 24 h. After completion of the reaction, cold anhydrous diethyl ether was added to produce a white precipitate. The crude product was purified by washing with DCM and collected by filtration to give a white solid (47 mg, 60%). ESI-MS m/z $[M+H]^+$ of RSSD conjugate: 1427.5807 (calculated 1428.3200), ESI-MS m/z $[M+H]^+$ of QSSD conjugate: 1482.1320 (calculated 1481.8000) (Figure S7).

All APDCs were also characterized by ^{1}H nuclear magnetic resonance spectroscopy (^{1}H NMR), fourier transform infrared spectroscopy (FTIR), Micro-Raman imaging spectrometer (Raman) and ultraviolet-visible spectrophotometer (UV-vis). The ^{1}H NMR spectra of APDCs are shown in Figure S5. All characteristic signals of DM1 and cRGDfK could be seen clearly in RCCD and RSSD conjugates. In addition, DM1 and cRPQfK could be seen clearly in QCCD and QSSD conjugates. After coupling reaction, the four proton signals of DM1 at 6.92 ppm (1) attributed to the benzene ring (-Ar<u>H</u>), 5.95 ppm (2), 5.56 ppm (3) and 5.33 ppm (4) attributed to the alkene (-C<u>H</u>=C<u>H</u>- and -C<u>H</u>=C-, cyclic olefinic bond) shifted to 6.90 ppm (1'), 5.96 ppm (2'), 5.56 ppm (3') and 5.31 ppm (4') in the ^{1}H NMR spectrum of RCCD, 6.91 ppm (1''), 5.95 ppm (2''), 5.57 ppm (3'') and 5.32 ppm (4'') in the ^{1}H NMR spectrum of RSSD, 6.94 ppm (1'''), 5.97 ppm (2'''), 5.56 ppm (3''') and 5.31 ppm (4''') in the ^{1}H NMR spectrum of QCCD, and 6.92 ppm (1''''), 5.94 ppm (2''''), 5.56 ppm (3'''') and 5.30 ppm (4'''') in the ^{1}H NMR spectrum of QSSD, respectively. The proton signals of cRGDfK at 8.45-7.17 ppm (a) belonging to the acylamino (-CO-N<u>H</u>-) and benzene ring (-Ar<u>H</u>) shifted to 8.45-7.18 ppm (a') and 8.36-7.16 ppm (a'') in the ^{1}H NMR spectra of RCCD and RSSD. Similarly, the proton signals of cRPQfK at 8.56-6.84 ppm (b) belonging to the acylamino (-CO-N<u>H</u>-) and benzene ring (-Ar<u>H</u>) shifted to 8.52-6.77 ppm (b') and 8.51-6.83 ppm (b'') in the ^{1}H NMR spectra of QCCD and QSSD, respectively.

The FTIR spectra of APDCs are presented in Figure S6. Compared with the FTIR spectrum of DM1, the absorption band at 2558 cm^{-1} related to the sulfydryl stretching vibration disappeared completely in the FTIR spectra of RCCD, RSSD, QCCD and QSSD conjugates. The other two C=O stretching absorption band of DM1 at 1746 cm^{-1} (belong to the linear ester) and 1709 cm^{-1} (belong to ring lactonic) moved

to 1739 cm^{-1} and 1703 cm^{-1} after coupling reaction with cRGDfK or cRPQfK by thioether linkage. But, the one C=O stretching absorption band of DM1 at 1746 cm^{-1} (belong to the linear ester) moved to 1733 cm^{-1}, while the another C=O stretching absorption band of DM1 at 1709 cm^{-1} (belong to ring lactonic) appeared as a wide stretching absorption band at 1639 ~ 1709 cm^{-1} after coupling reaction with cRGDfK or cRPQfK by disulfide linkage.

The raman spectra of maytansinoid DM1, cRGDfK, RCCD conjugate, RSSD conjugate, cRPQfK, QCCD conjugate and QSSD conjugate are shown in Figure S8A. The stretching absorption bands of free DM1 and cRGDfK can be seen clearly in RCCD and RSSD conjugates, and the stretching absorption bands of free DM1 and cRPQfK can be seen clearly in QCCD and QSSD conjugates. After coupling reaction, compared with the raman spectra of free DM1, a strong S-H stretching absorption band at 2571 cm^{-1} related to the thiol group disappears completely. As shown in Figure S8B, a wide S-S stretching absorption band appears at 670-636 cm^{-1} in all conjugates. In addition, a wide S-S stretching absorption band appears at 500-550cm^{-1} in RSSD and QSSD conjugates. These raman results demonstrate that the RCCD, RSSD, QCCD and QSSD conjugates are synthesized successfully.

In Figure S9A, both UV-vis absorption bands of DM1 and cRGDfK can be seen clearly in the RCCD and RSSD conjugates, and the QCCD and QSSD conjugates possesses both UV-vis absorption bands of DM1 and cRPQfK. After coupling reaction, these changes of the maximum emission peak and peak shape are observed in the UV-vis spectrum of RCCD, RSSD, QCCD and QSSD conjugates compared with the UV-vis absorption of free DM1 (as shown in Figure S9B). In addition, a new absorption peak at 339 nm appears in the RSSD and QSSD conjugates. The UV-vis results further confirm the successful conjugation between peptide and maytansinoid

DM1. All experiments demonstrated the successful synthesis of four types of designed APDCs.

1.3 Interaction between Various APDC@NPs and Integrin αvβ3 Detected by Surface Plasmon Resonance (SPR) Technology

A SPR assay was performed at 25 °C via a BIACORE T3000 instrument (BIACORE T3000, GE Healthcare) equipped with a CM-5 chip to investigate the integrin αvβ3 binding affinity of the APDC@NPs [4]. Briefly, the surface of the sensor chip was first activated by 1-ethyl-3-[3-dimethylaminopropyl] carbodiimide hydrochloride (EDC) and *N*-hydroxysuccinimide (NHS). Next, integrin αvβ3 was covalently linked onto the chip, followed by acetamide blocking. When the response (RU) signal was stabilized, different APDC@NPs' solution were injected into the chamber, and the binding process was monitored with a flow rate of 5 μL min^{-1} for 1 min. Before each injection, the phosphate buffer was used to wash APDC@NPs off the sensor chip. As exhibited in Figure S16, via SPR technology, we demonstrated that the active targeting RCCD@NPs and RSSD@NPs enhanced the interaction between nanoparticles and integrin αvβ3.

1.4 Cell culture

B16 mouse melanoma cells and MCF-7 human breast cancer cells were cultured in RPMI-1640 while HUVEC endothelial cells were cultured in Ham's F12K-Medium. All the cell lines were provided by the Institute of Basic Medical Science, Chinese Academy of Medical Science and grew at the culture media contain 10% fetal bovine serum (FBS) and antibiotics (100 U mL^{-1} penicillin and 100 U mL^{-1} streptomycin) at 37 ^{o}C under a humidified atmosphere containing 5% CO_2.

1.5 Preparation and Characterization of Various Cy3.5-loaded APDC@NPs

The typical procedure was used to prepare various Cy3.5-loaded APDC@NPs

[5]. Briefly, 4.5 mg APDC conjugate was dissolved in 1.0 mL DMSO, followed by adding a 0.2 mL of Cy3.5 solution (1 mg/mL) in DMSO and stirred at room temperature for 10 min. Then the mixture was slowly added into 3.0 mL of deionized water and stirred slightly for another 10 min. Subsequently, the solution was dialyzed against deionized water for 18 h (MWCO 1000 Da) and the deionized water was exchanged for 8 times. Then the Cy3.5-loaded APDC@NPs' solution was lyophilized and then dissolved in DMSO again in order to determine the amount of Cy3.5. The Cy3.5 content in APDC@NPs was determined by the absorbance at 581 nm measured using a fluorescence spectrophotometer. The particle size and PDI of various Cy3.5-loaded APDC@NPs were measured in triplicate by a dynamic light scattering (DLS) analysis using a Malvern Zetasizer Nano ZS (Malvern, Malvern, United Kingdom) at 25 ^{o}C. Figure S21 gives the size distribution of the Cy3.5-loaded APDC@NPs, their average size and polydispersity index. Both size and polydispersity index of Cy3.5-loaded APDC@NPs are very similar to those of APDC@NPs without Cy3.5 (Figure 1A).

1.6 Immunofluorescence for Integrin αvβ3 Expression

B16, MCF-7 or HUVEC cells were cultured on glass-bottom dishes for 24 h at 37 °C, respectively. The cells were fixed with 4% (v/v) paraformaldehyde for 15 min at 37 °C, and washed with PBS for three times. Then, cells were blocked with 5% BSA for 1 h at room temperature, followed by incubated with murine monoclonal antibodies to integrin alpha v beta 3 (Abcam, UK). Negative controls (PBS added) were included. The secondary antibody consisted of Alexa Fluor® 647 dye-conjugated Affinipure Goat Anti-rabbit was incubated with cells for 1 h 37 °C. Cell nuclei were stained with Hoechst 33258, and the samples were observed using a Leica TCS SP5 confocal laser-scanning microscope (CLSM, Heidelberg, Germany).

All the immunofluorescence experiments were performed at least three times. Integrin αvβ3 expression in B16 and HUVEC cells was confirmed by immunofluorescence with MCF-7 cells as a negative control. As shown in Figure S22, strong binding of Alexa Fluor® 647 dye-labeled secondary antibody was observed in B16 and HUVEC cells, and the fluorescence intensity in B16 cells was comparable to HUVEC cells, however, the fluorescence intensity in MCF-7 cells was obviously lower compared with other two cell lines. Thus, B16 and HUVEC cells highly expressed integrin αvβ3, while MCF-7 cells exhibited little αvβ3 expression.

1.7 Animals

All C57BL/6 mice (female, 6-8 weeks) were provided by Peking University Health Science Center and kept under SPF conditions with free access to standard food and water. All the studies complied with the principles of care and use of laboratory animals and were approved by the Institutional Animal Care and Use Committee of Peking University.

1.8 TUNEL Analysis

Frozen sections made from tumors of each group were used to evaluate apoptosis of tumor cells by terminal deoxynucleotide transferase (TdT)-mediated dUTP-biotin nickend labeling (TUNEL) assay, using the manufacturer's protocol from the in situ cell apoptosis detection kit. Briefly, the tumor samples were frozen in optimal cutting temperature (O.C.T.) embedding medium, cut into 5 mm sections, and stored at -20 °C before use. The tumor sections were fixed in 4% paraformaldehyde for 20 min and washed with PBS thrice. Then 0.1% triton X-100 was added to permeabilize the cells for 4 min at room temperature. The sections were incubated in TUNEL equilibration buffer containing reaction mixture in a dark humidified box for 1 h at 37 °C. The sections were then washed with PBS thrice to remove the unincorporated

Streptavidin-FITC, and further incubated with Hoechst 33258 for another 30 min. The samples were finally imaged through CLSM with DNA strand breaks shown in green and cell nuclei in blue, respectively.

1.9 Immunohistochemical Analysis

Immunohistochemical staining [6] was performed on paraffin sections of B16 tumors that were dissected from each mouse of six treatment groups on day 25. The tumor sections were stained with rabbit primary antibody against CD31, and then the expression of platelet endothelial cell adhesion molecule-1 (CD31) of each section was observed under CLSM to evaluate the tumor angiogenesis. Moreover, the expression of Antigen Ki-67 was observed under CLSM to evaluate the cell proliferation in each tumor sample.

2. References

1. Chari RVJ, Martell BA, Gross JL, et al. Immunoconjugates Containing Novel Maytansinoids: Promising Anticancer Drugs. Cancer Res. 1992; 52: 127-131.
2. Mei D, Lin Z, Fu J, et al. The use of α-conotoxin ImI to actualize the targeted delivery of paclitaxel micelles to α7 nAChR-overexpressing breast cancer. Biomaterials. 2015; 42: 52-65.
3. Chuan X, Song Q, Lin J, et al. Novel Free-Paclitaxel-Loaded Redox-Responsive Nanoparticles Based on a Disulfide-Linked Poly(ethylene glycol)-Drug Conjugate for Intracellular Drug Delivery: Synthesis, Characterization, and Antitumor Activity in Vitro and in Vivo. Mol Pharm. 2014; 11: 3656-3670.
4. Guo Z, He B, Jin H, et al. Targeting Efficiency of RGD-modified Nanocarriers with Different Ligand Intervals in Response to Integrin αvβ3 Clustering. Biomaterials. 2014; 35: 6106-6117.
5. Huang P, Wang D, Su Y, et al. Combination of Small Molecule Prodrug and

Nanodrug Delivery: Amphiphilic Drug−Drug Conjugate for Cancer Therapy. J Am Chem Soc. 2014; 136: 11748-11756.

6. Wang Y, Yang T, Wang X, et al. Materializing sequential killing of tumor vasculature and tumor cells via targeted polymeric micelle system. J Control Release. 2011; 149: 299-306.

3. Table

Table S1 The IC_{50} value of free DM1 and various APDC@NPs with or without pre-treatment of GSH-OEt on various cell lines for 48 h by SRB method (n=3).

		IC_{50}/nM		
		B16	MCF-7	HUVEC
DM1		32.26±8.36	52.48±9.82	12.88±1.92
RCCD@NPs	-	102.33±38.92	407.38±54.05	33.84±6.30
	+GSH-OEt	91.20±12.86	489.77±62.65	42.66±8.91
QCCD@NPs	-	389.05±75.25	331.13±85.56	67.61±13.67
	+GSH-OEt	371.54±30.25	354.81±40.92	85.11±12.04
RSSD@NPs	-	21.38±4.32	302.00±72.91	20.42±4.70
	+GSH-OEt	5.09±1.22 **	32.20±12.63 ##	12.02±3.15 &&
QSSD@NPs	-	245.47±37.54	371.53±94.49	154.88±31.85
	+GSH-OEt	147.91±46.79 *	48.80±15.94 ##	63.10±18.96 &

*$p < 0.05$ and **$p < 0.01$ versus the cell viability of B16 cells without pre-treatment of GSH-OEt, $^{\#\#}p < 0.01$ versus the cell viability of MCF-7 cells without pre-treatment of GSH-OEt, $^{\&}p < 0.05$ and $^{\&\&}p < 0.01$ versus the cell viability of HUVEC cells without pre-treatment of GSH-OEt.

4. Figures

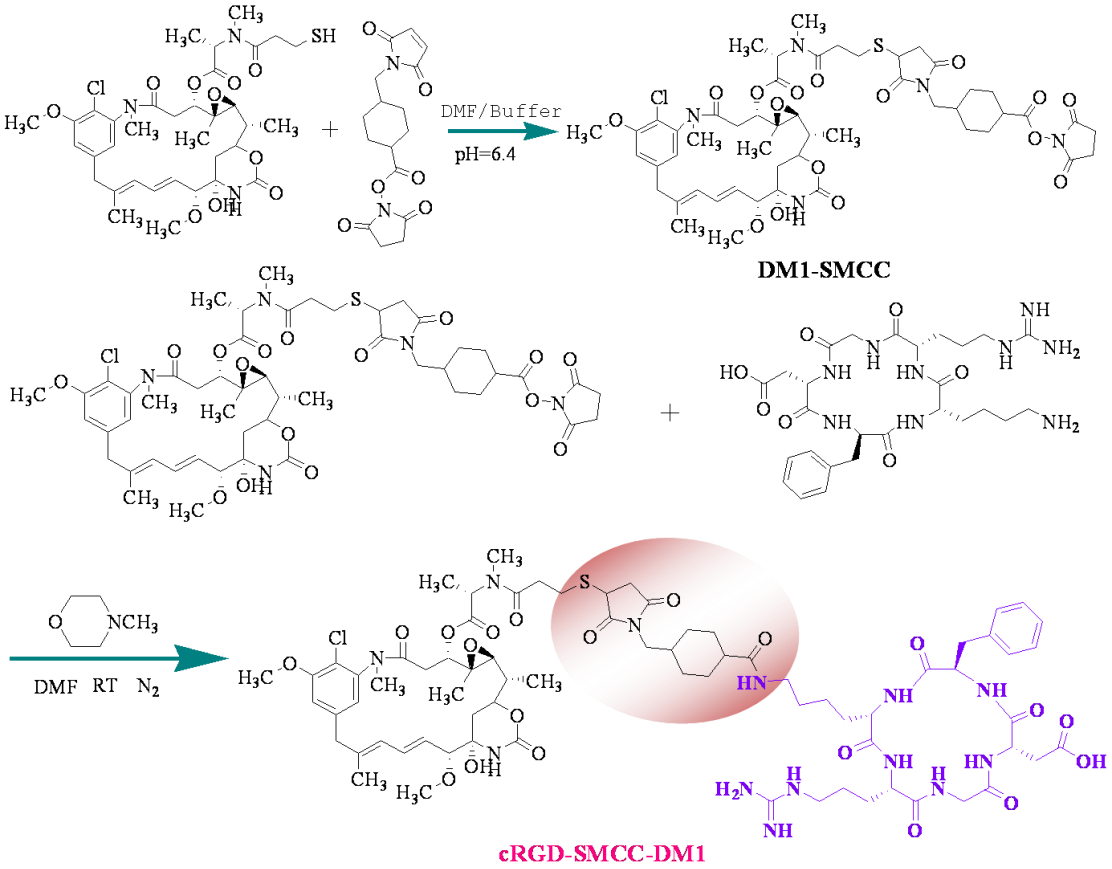

Figure S1. Synthetic routes of the amphiphilic thioether-linked cRGD-SMCC-DM1 (RCCD) conjugate.

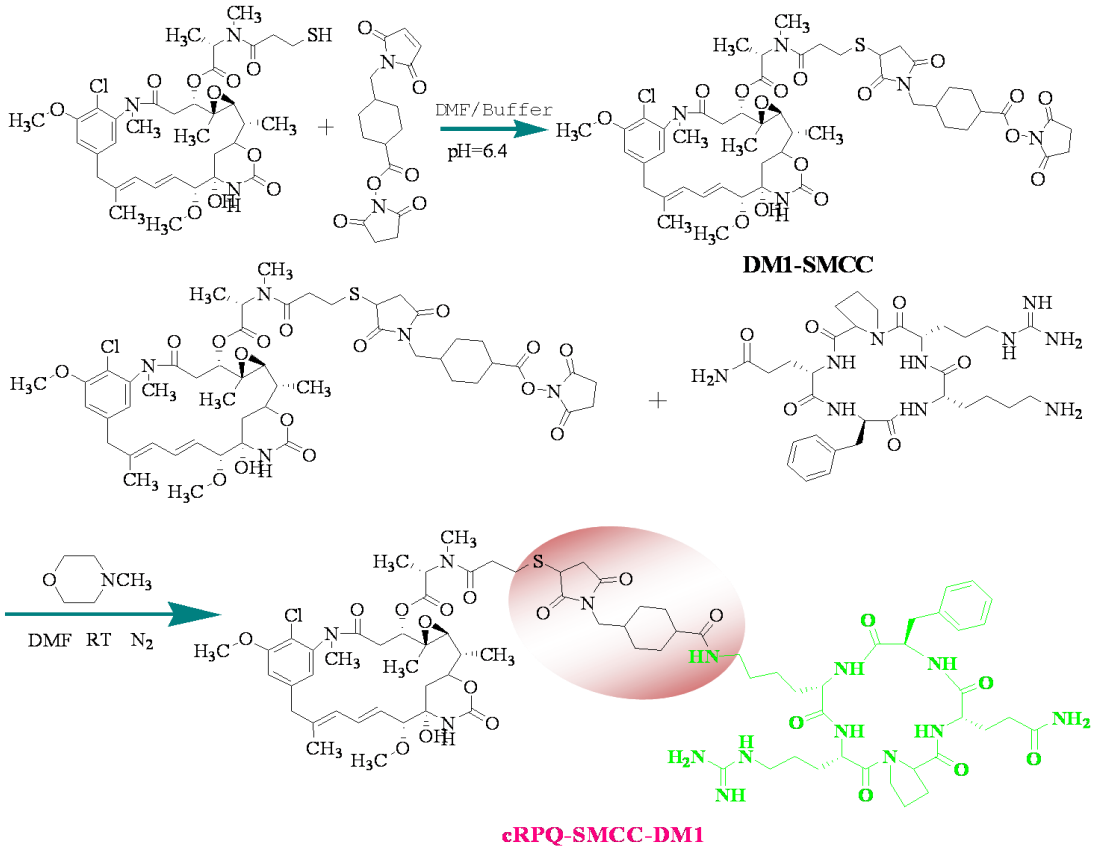

Figure S2. Synthetic routes of the amphiphilic thioether-linked cRPQ-SMCC-DM1 (QCCD) conjugate.

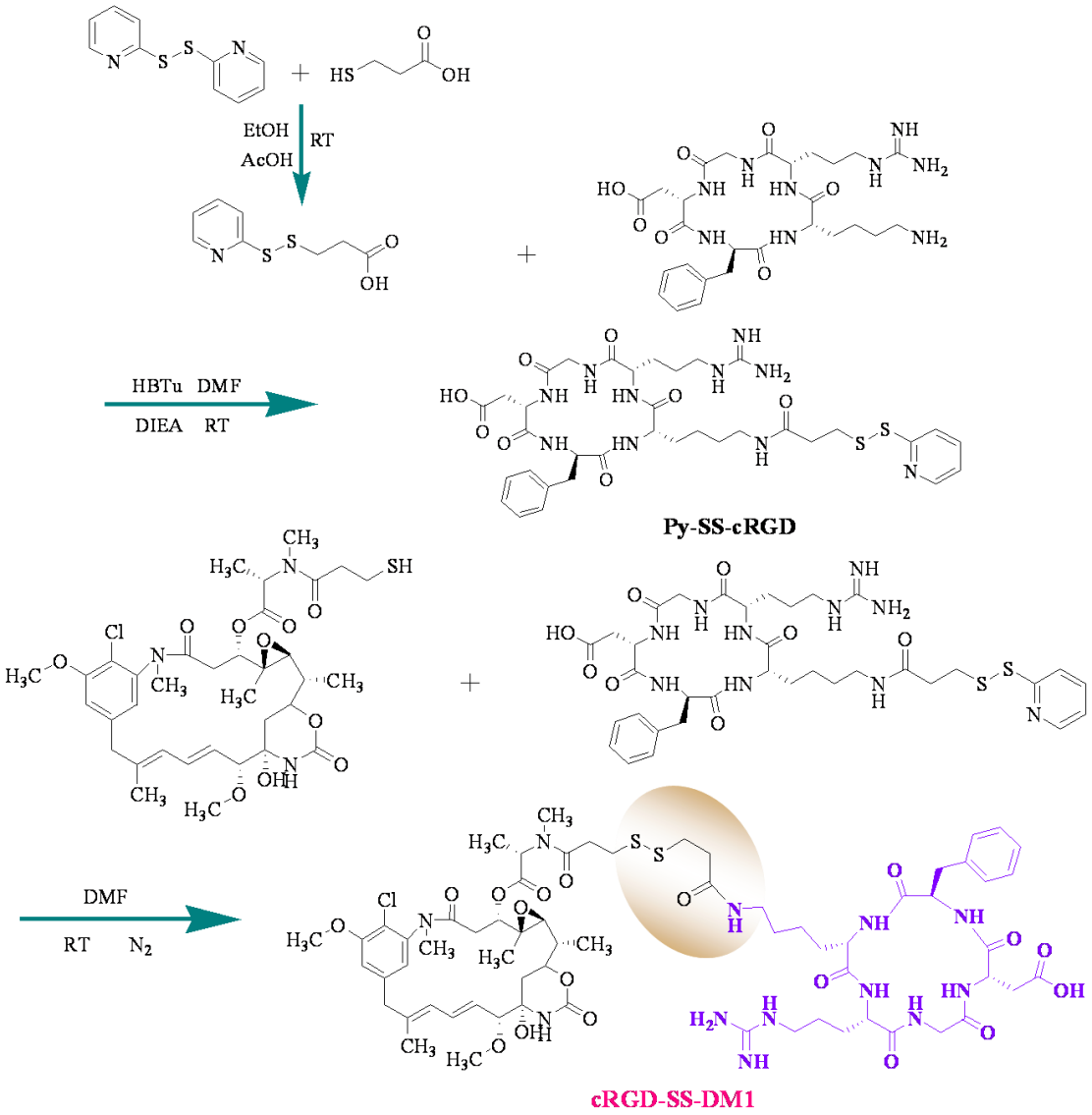

Figure S3. Synthetic routes of the amphiphilic disulfide-linked cRGD-SS-DM1 (RSSD) conjugate.

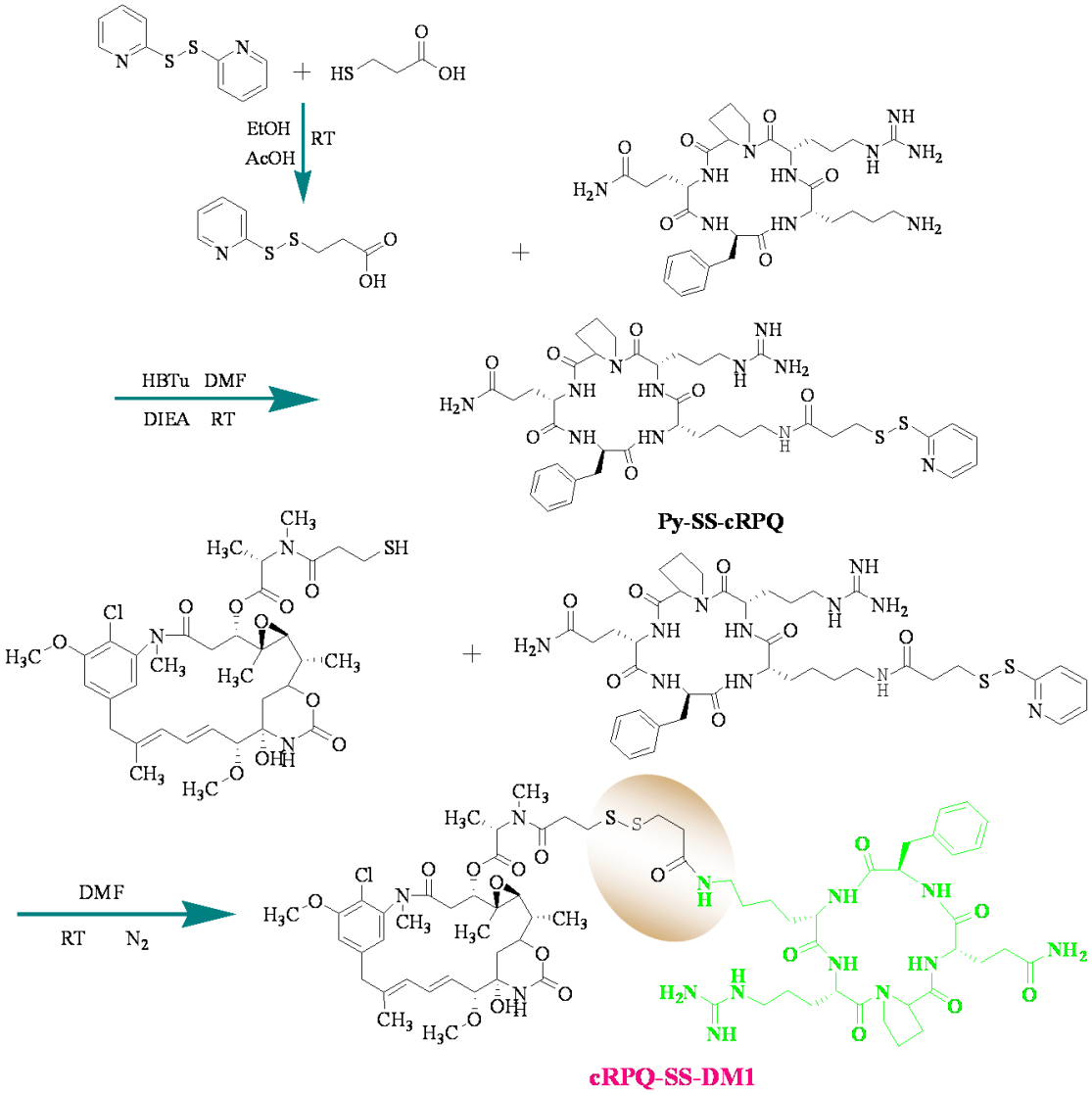

Figure S4. Synthetic routes of the amphiphilic disulfide-linked cRPQ-SS-DM1 (QSSD) conjugate.

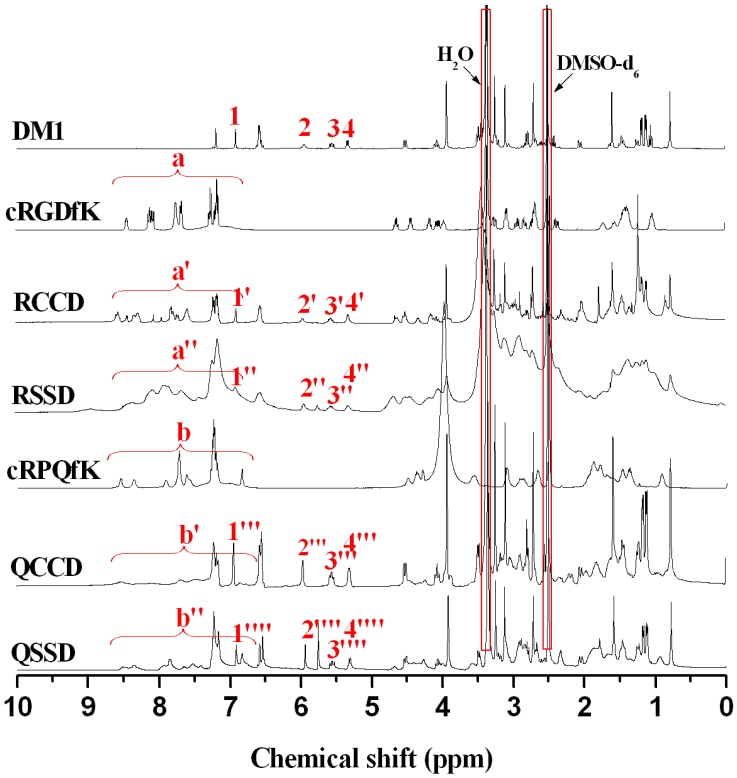

Figure S5. ^{1}H NMR spectra of DM1, cRGDfK, RCCD conjugate, RSSD conjugate, cRPQfK, QCCD conjugate and QSSD conjugate in DMSO-d_6.

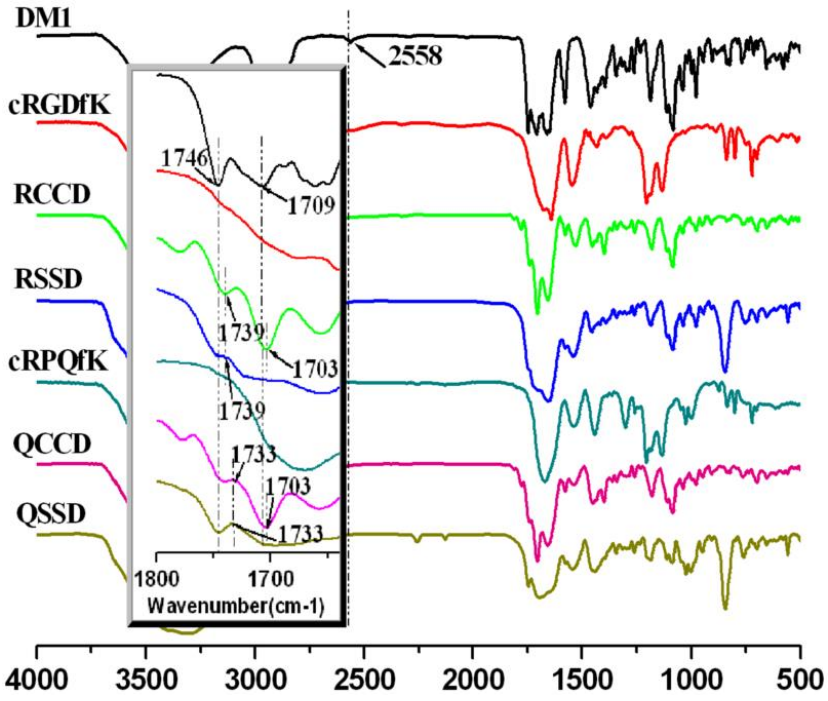

Figure S6. FTIR spectra of DM1, cRGDfK, RCCD conjugate, RSSD conjugate, cRPQfK, QCCD conjugate and QSSD conjugate.

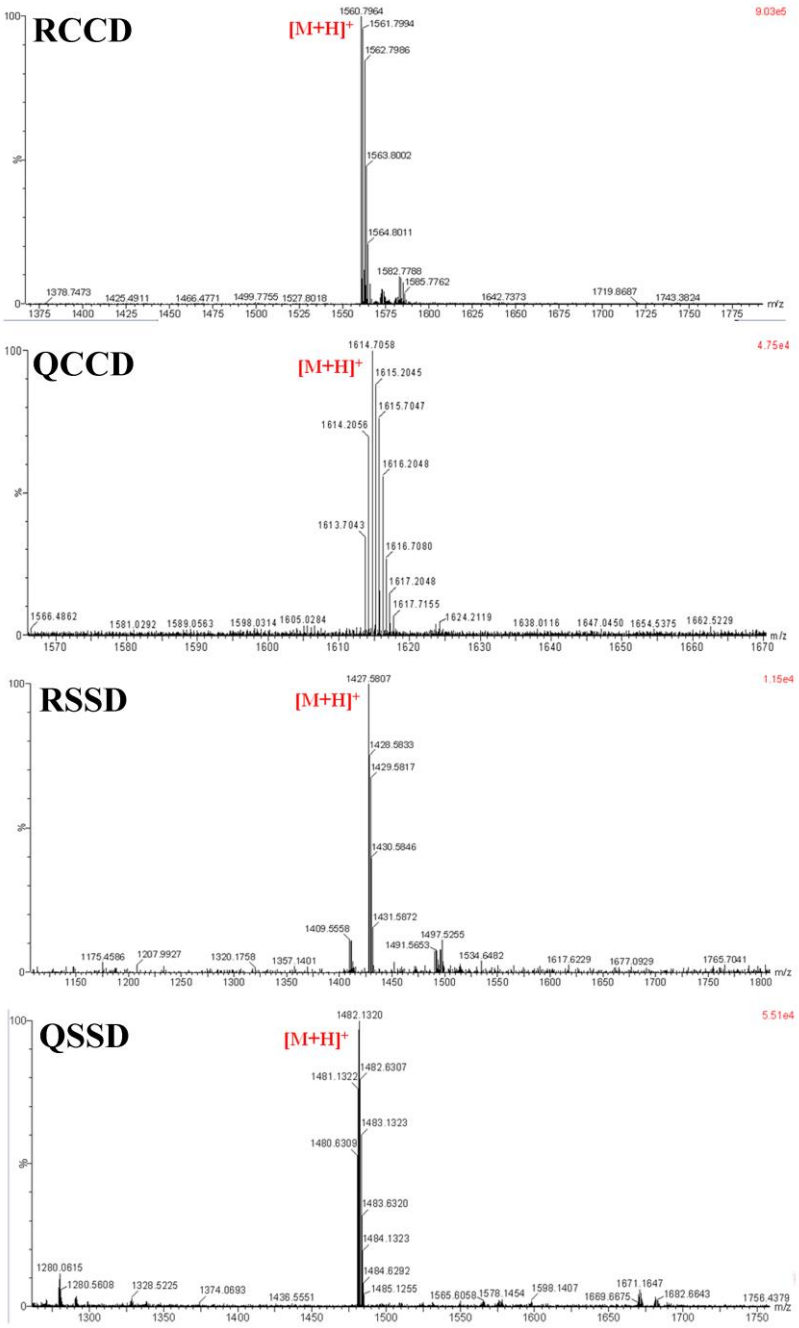

Figure S7. ESI-MS spectra of RCCD, QSSD, QCCD and RSSD conjugates.

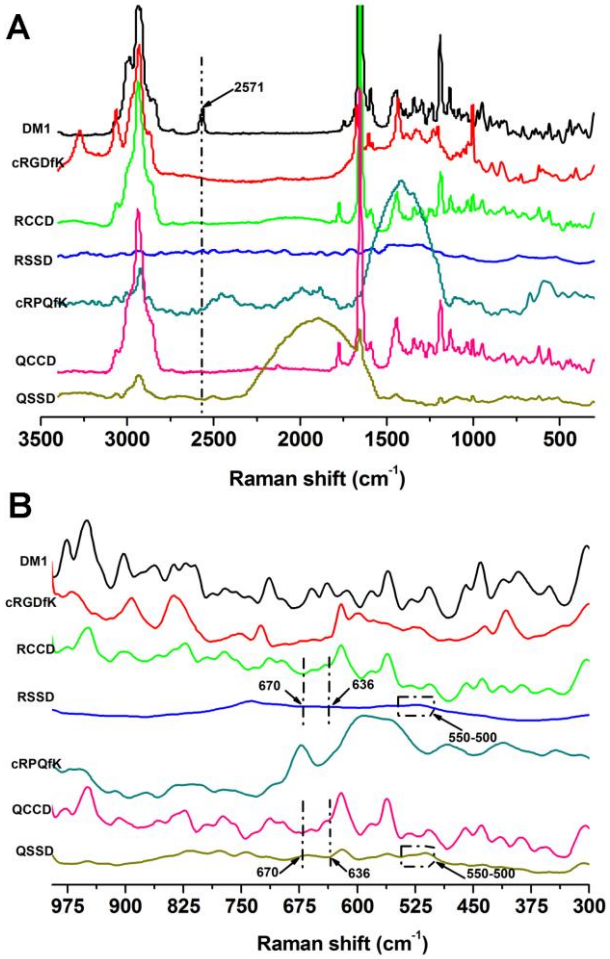

Figure S8. (A) Raman spectra of maytansinoid DM1, cRGDfK, RCCD conjugate, RSSD conjugate, cRPQfK, QCCD conjugate and QSSD conjugate. (B) A partial raman spectra of maytansinoid DM1, cRGDfK, RCCD conjugate, RSSD conjugate, cRPQfK, QCCD conjugate and QSSD conjugate in the range of 300 ~ 1000 cm^{-1}.

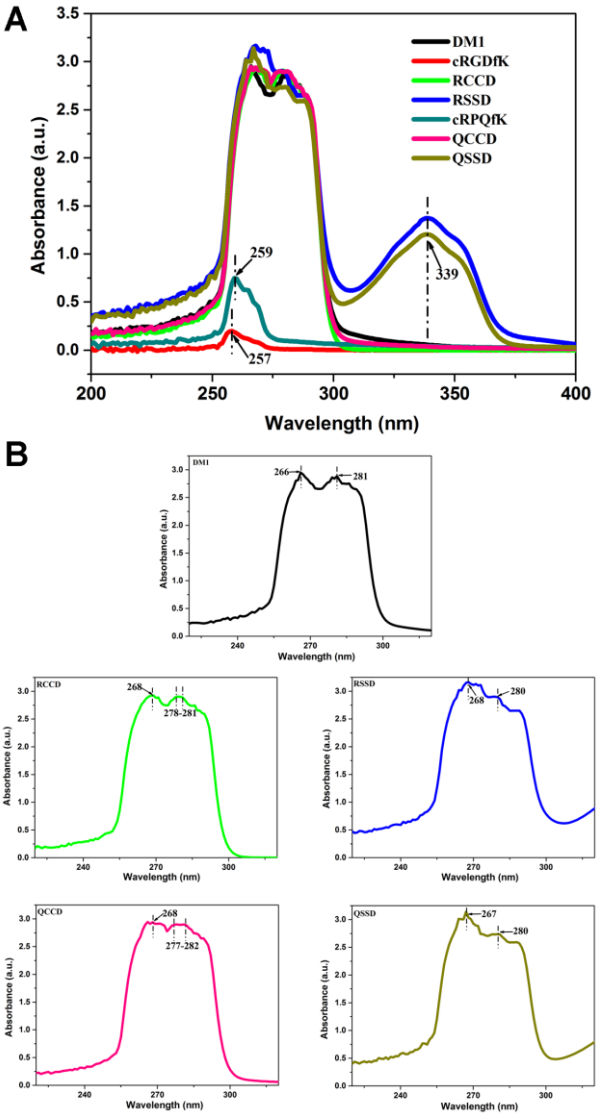

Figure S9. (A) UV-vis spectra of maytansinoid DM1, cRGDfK, RCCD conjugate, RSSD conjugate, cRPQfK, QCCD conjugate and QSSD conjugate in dimethyl sulfoxide. (B) A partial UV-vis spectra of DM1, RCCD, RSSD, QCCD and QSSD conjugates in the range of 220 ~ 320 nm.

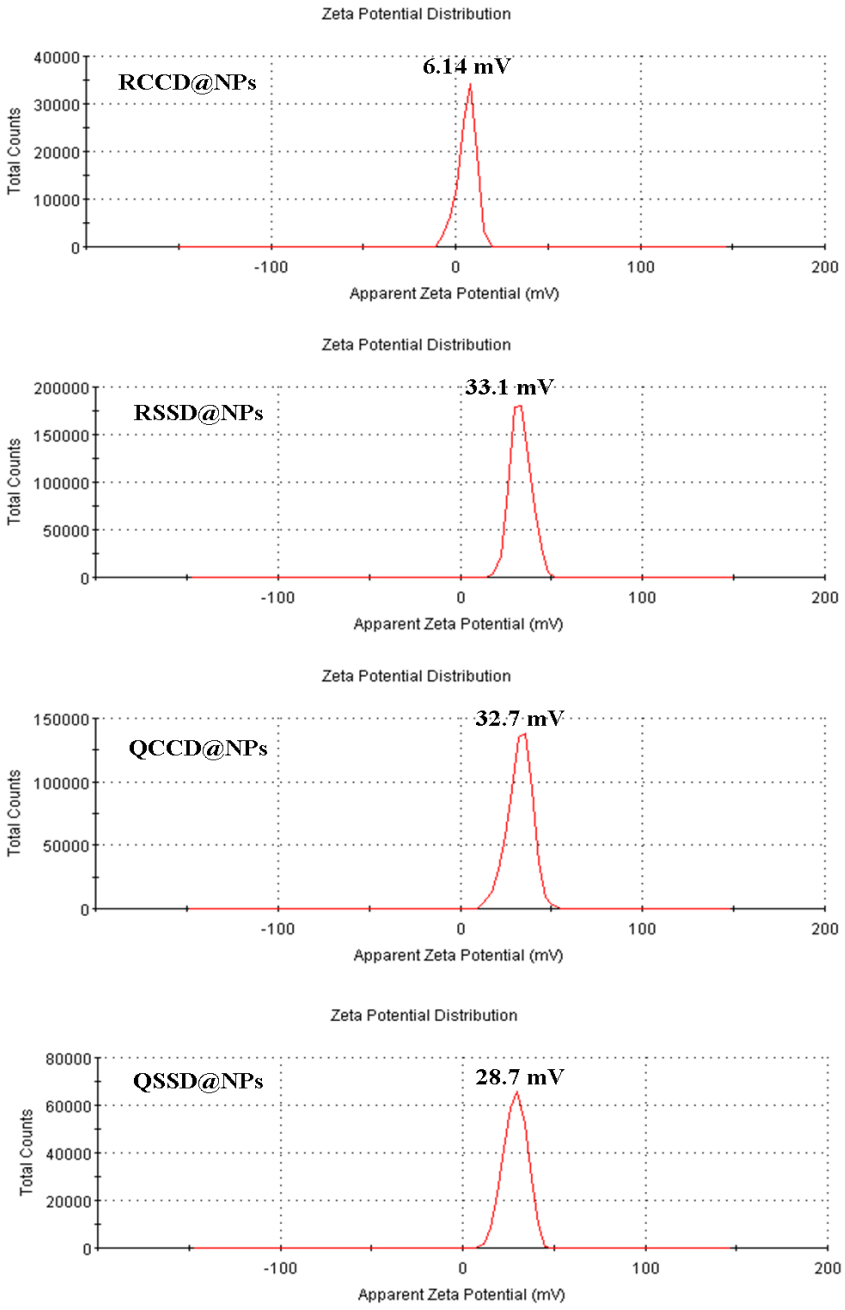

Figure S10. The zeta potential ($Zeta_{RCCD}$=6.14mV, $Zeta_{RSSD}$=33.1mV, $Zeta_{QCCD}$=32.7mV, $Zeta_{QSSD}$=28.7mV) of various APDC@NPs by Zetasizer.

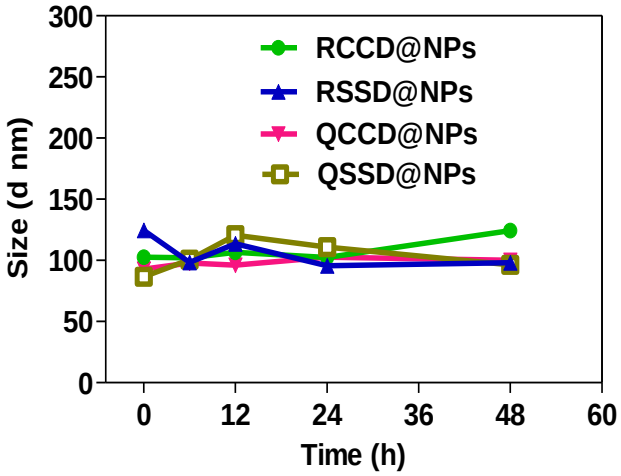

Figure S11. Size changes of various APDC@NPs in serum at 37 °C.

In the Figure S11, no significant change in the diameter of various APDC@NPs was observed for more than 48 h in serum at 37 °C, which suggests that the prepared APDC@NPs may reach the tumor in intact form through the blood circulation.

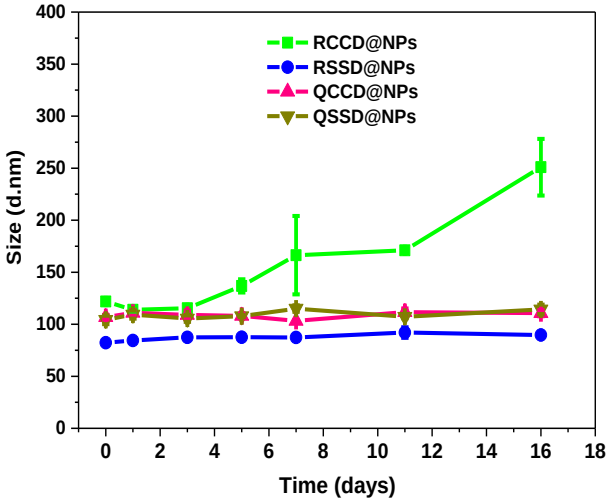

Figure S12. The particle size of APDC@NPs during the storage at 4 °C. The aqueous solutions of APDC@NPs were stored at 4 °C in refrigerator for 16 days. At different time intervals (0, 1, 3, 5, 7, 11 and 16 d), the average size were determined by DLS. Samples were measured in triplicates. The values are the mean ± SD.

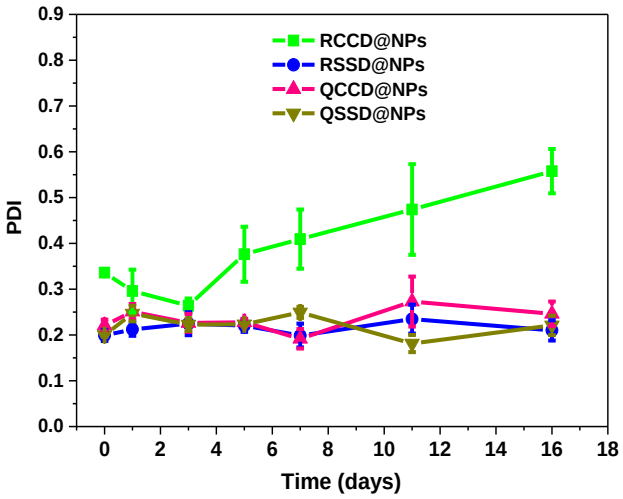

Figure S13. The polydispersity indexes (PDI) of particle size of APDC@NPs during the storage at 4 °C. The aqueous solutions of APDC@NPs were stored at 4 °C in refrigerator for 16 days. At different time intervals (0, 1, 3, 5, 7, 11 and 16 d), the PDI were determined by DLS. Samples were measured in triplicates. The values are the mean ± SD.

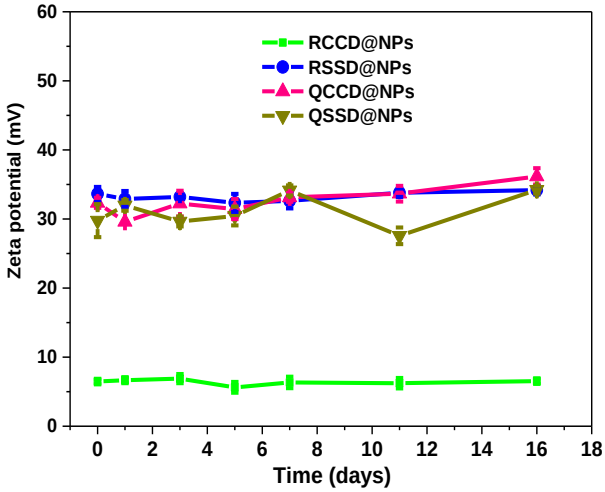

Figure S14. The zeta potential of APDC@NPs during the storage at 4 °C. The aqueous solutions of APDC@NPs were stored at 4 °C in refrigerator for 16 days. At different time intervals (0, 1, 3, 5, 7, 11 and 16 d), the zeta potential were determined by DLS. Samples were measured in triplicates. The values are the mean ± SD.

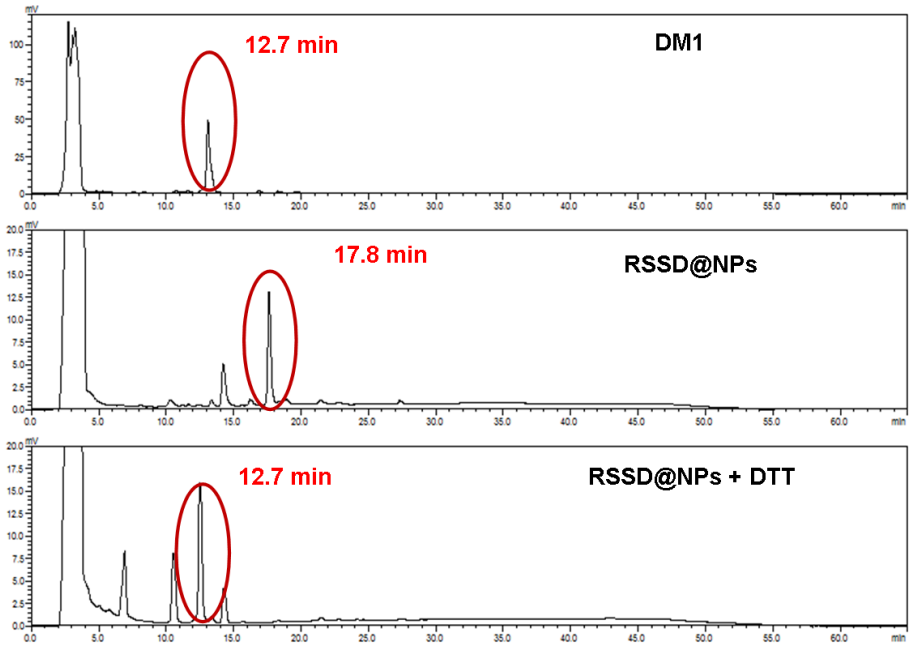

Figure S15. HPLC chromatogram of DM1, RSSD@NPs with or without the presence of reducing agent DTT at 37 °C in PBS (pH 7.4, n = 3) for 24 h.

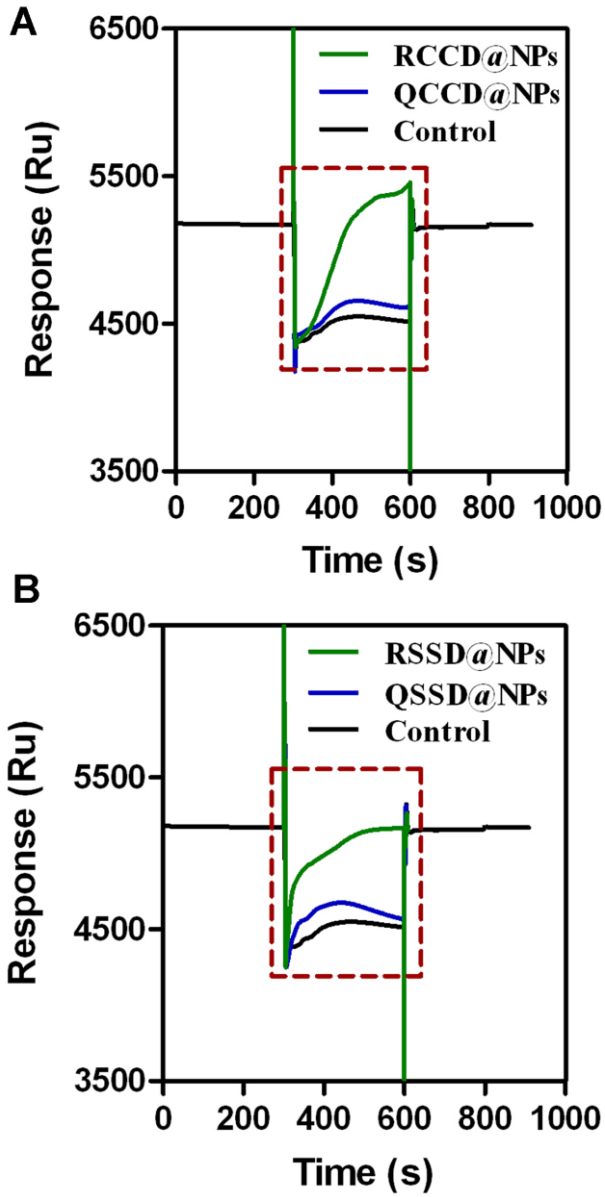

Figure S16. SPR responses to the interaction between APDC@NPs and integrin αvβ3 molecules. (A) SPR response of RCCD@NPs and QCCD@NPs group with integrin αvβ3 during a 1-min injection. (B) SPR response of RSSD@NPs and QSSD@NPs group with integrin αvβ3 during a 1-min injection. Dotted-line square frames indicate the area of response (RU).

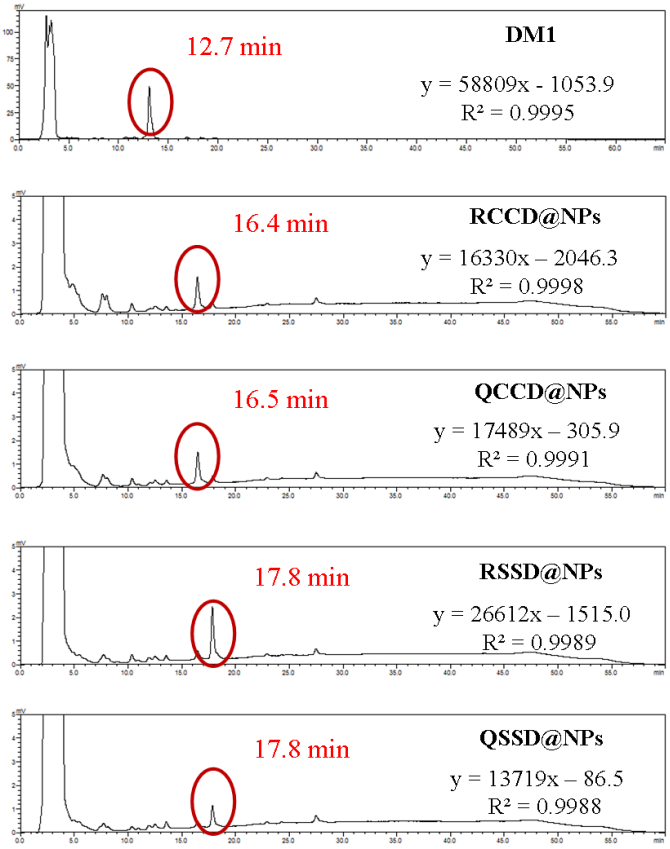

Figure S17. HPLC chromatogram of DM1, RCCD@NPs, QCCD@NPs, RSSD@NPs and QSSD@NPs.

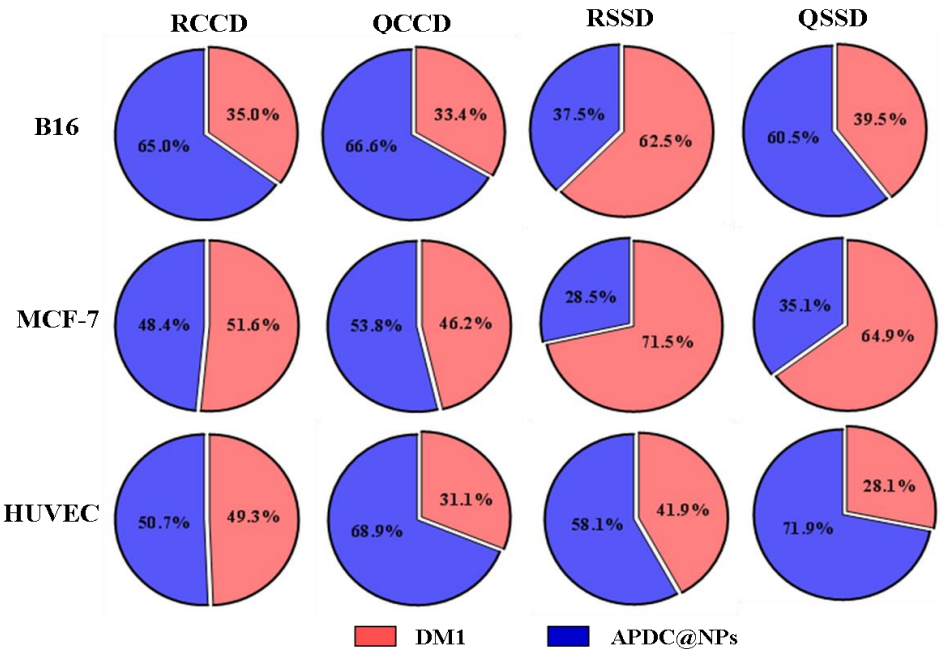

Figure S18. The percentage of intracellular DM1 and APDC@NPs determined by HPLC in B16, MCF-7 and HUVEC cells after treatments with different APDC@NPs at a drug dose of 100 nM (calculated by DM1) for 3 h (n=3). The total amount of DM1 and APDC@NPs are taken as 100%.

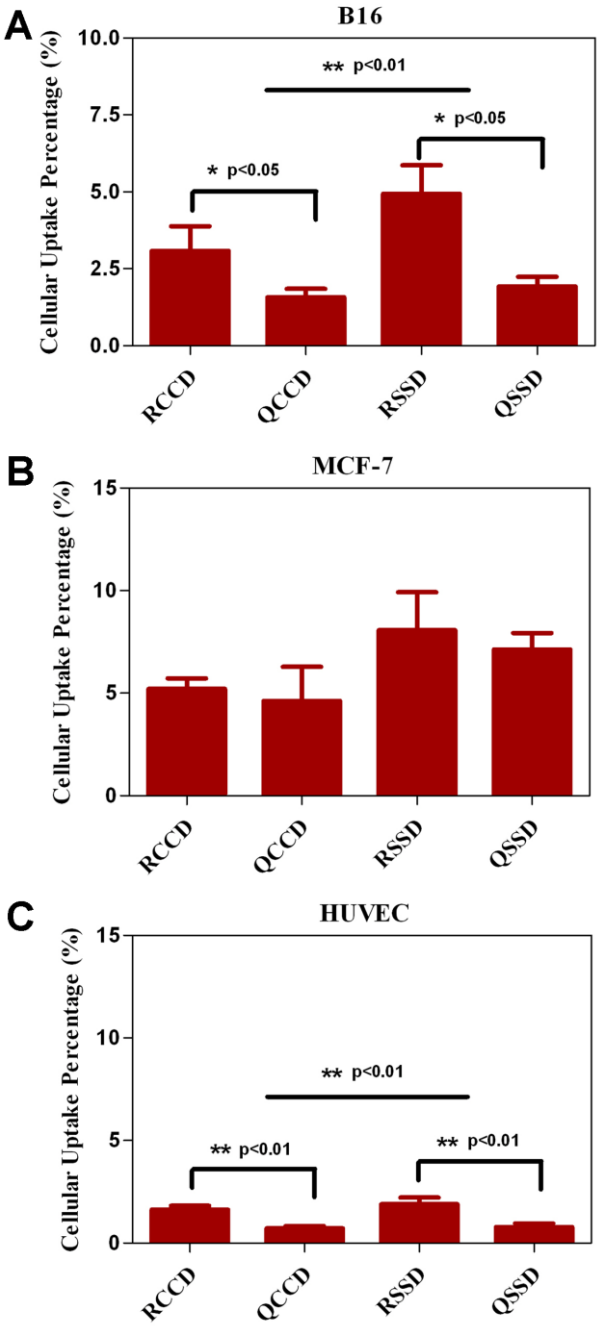

Figure 19. Intracellular concentrations of DM1 determined by HPLC in (A) B16 cells, (B) MCF-7 cells, and (C) HUVEC after treatments with different APDC@NPs at a drug dose of 100 nM for 3 h (n=3). **p < 0.01 versus the uptake of passive cRPQfK group or the thioether-linked nanosystems.

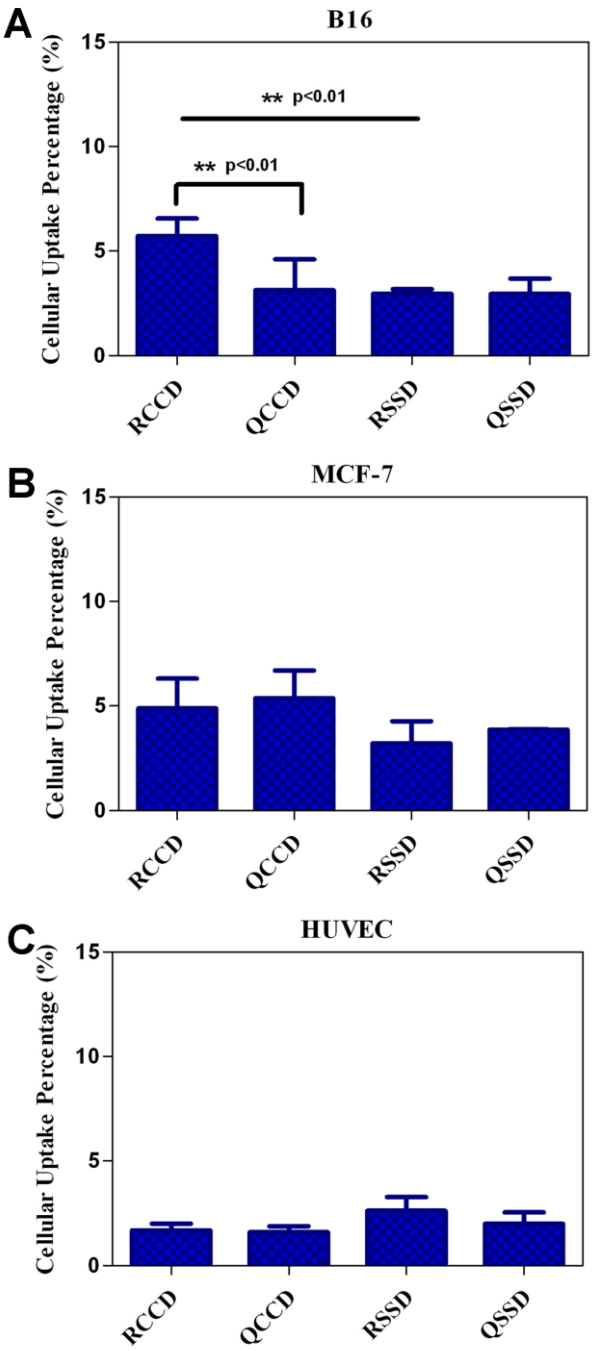

Figure 20. Intracellular concentrations of APDC@NPs determined by HPLC in (A) B16 cells, (B) MCF-7 cells, and (C) HUVEC after treatments with different APDC@NPs at a drug dose of 100 nM for 3 h (n=3). **p < 0.01 versus the uptake of passive cRPQfK group or the disulfide -linked nanosystems.

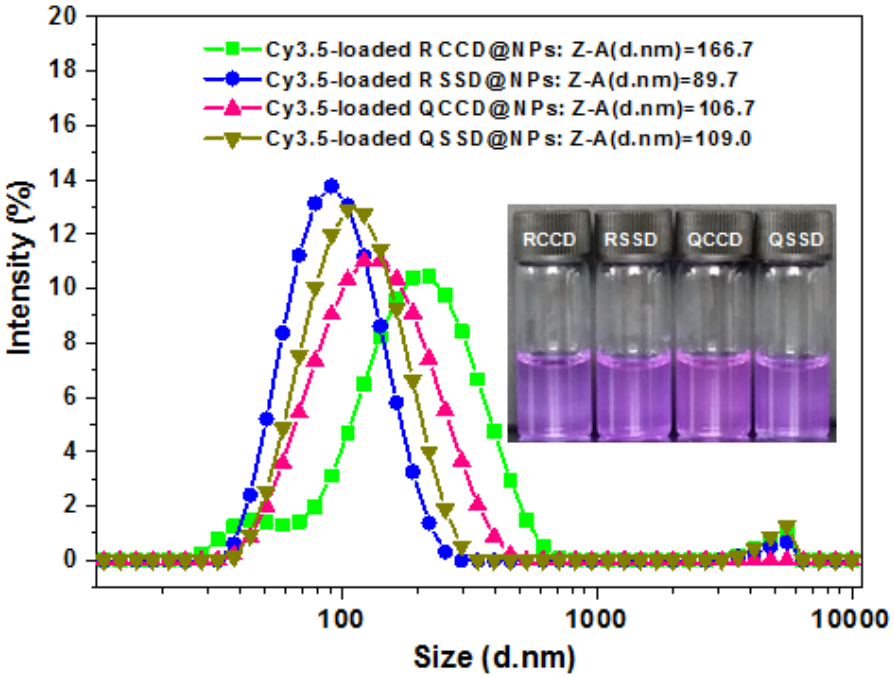

Figure S21. The size distribution of Cy3.5-loaded APDC@NPs by DLS analysis with the average hydrodynamic size (D_{RCCD}= 166.7 nm, D_{RSSD}= 89.7 nm, D_{QCCD}= 106.7 nm, D_{QSSD}= 109.0 nm) and the polydispersity index (PDI_{RCCD}= 0.331 nm, PDI_{RSSD}= 0.184 nm, PDI_{QCCD}= 0.281 nm, PDI_{QSSD}= 0.229 nm). Inset: The digital photographs of Cy3.5-loaded APDC@NPs' solution.

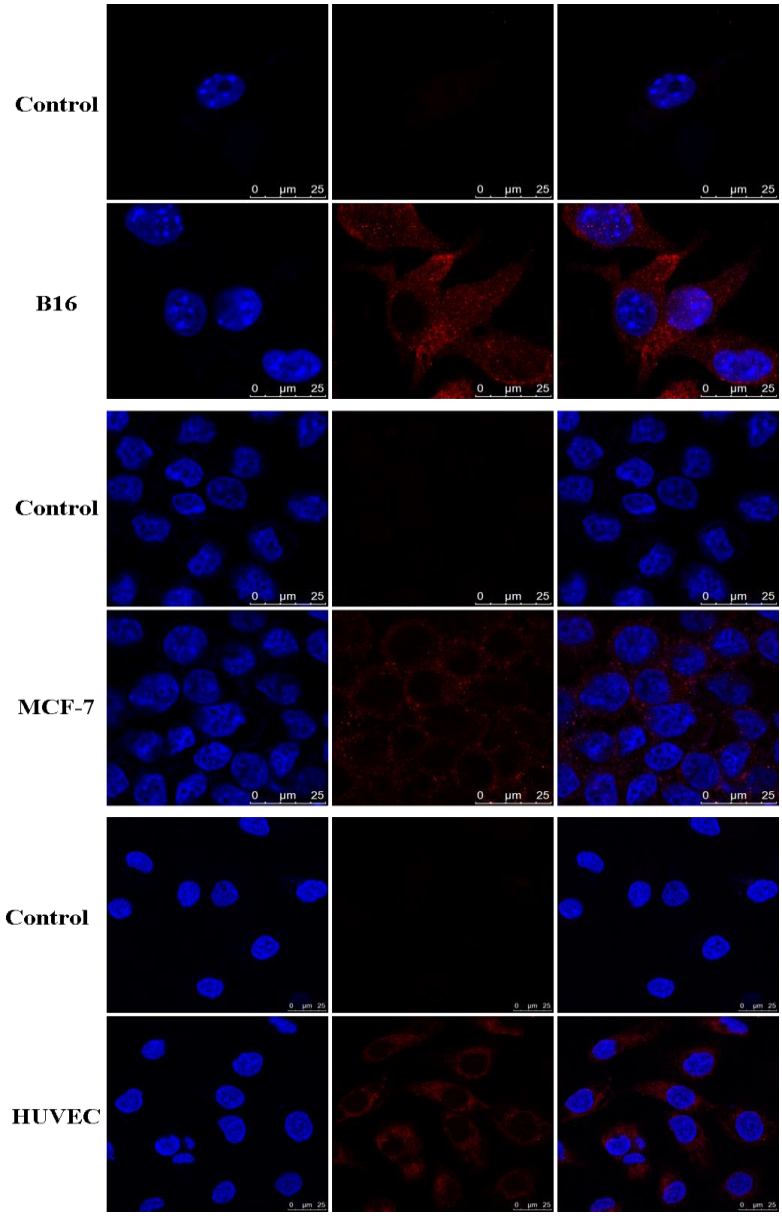

Figure S22. Integrin αvβ3 expression in B16 cells, MCF-7 cells and HUVEC cells. Cells without primary antibody incubation were used as a control. Red represents integrin alpha v beta 3 staining. Blue represents Hoechst 33258 fluorescence.

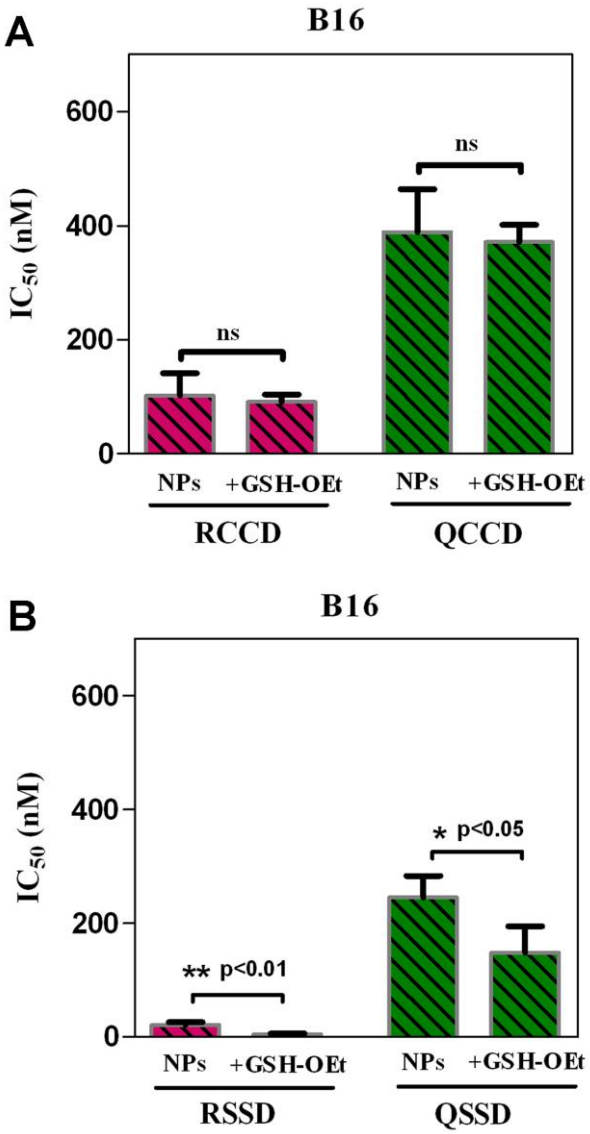

Figure S23. The IC_{50} value of (A) RCCD and QCCD nanoparticles, (B) RSSD and QSSD nanoparticles with or without pre-treatment of GSH-OEt on B16 cells for 48 h by SRB method (n=3). *p < 0.05, **p < 0.01 versus the cell viability of various cell lines without pre-treatment of GSH-OEt.

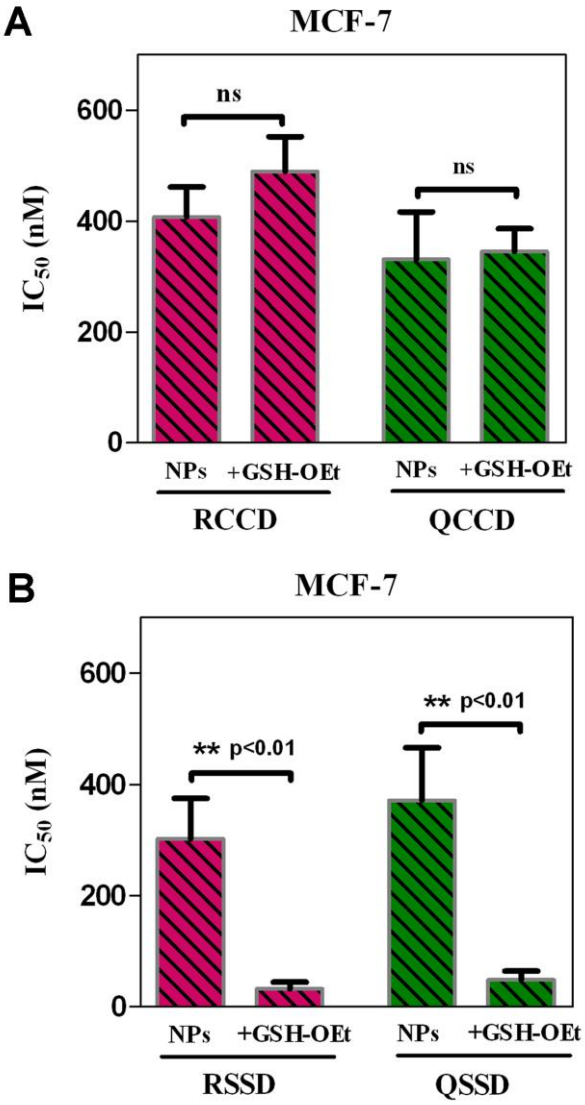

Figure S24. The IC_{50} value of (A) RCCD and QCCD nanoparticles, (B) RSSD and QSSD nanoparticles with or without pre-treatment of GSH-OEt on MCF-7 cells for 48 h by SRB method (n=3). *$p < 0.05$, **$p < 0.01$ versus the cell viability of various cell lines without pre-treatment of GSH-OEt.

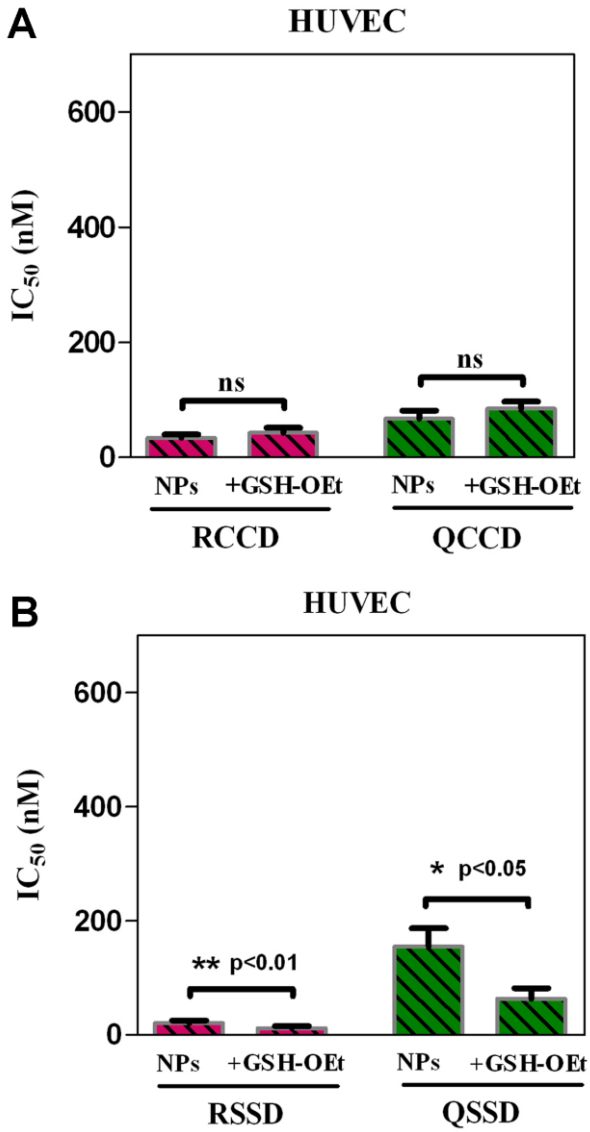

Figure S25. The IC_{50} value of (A) RCCD and QCCD nanoparticles, (B) RSSD and QSSD nanoparticles with or without pre-treatment of GSH-OEt on HUVEC cells for 48 h by SRB method (n=3). *p < 0.05, **p < 0.01 versus the cell viability of various cell lines without pre-treatment of GSH-OEt.

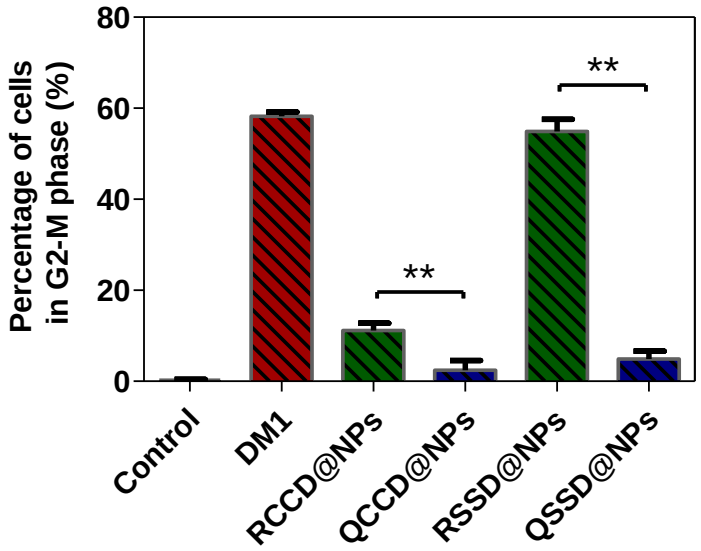

Figure S26. The percentage of cells in G2-M phase with different treatments of APDC@NPs at a drug dose of 50 nM (calculated by free DM1) for 12 h on B16 cells (n=3). *p < 0.05, **p < 0.01, p = ns versus the passive cRPQfK groups.

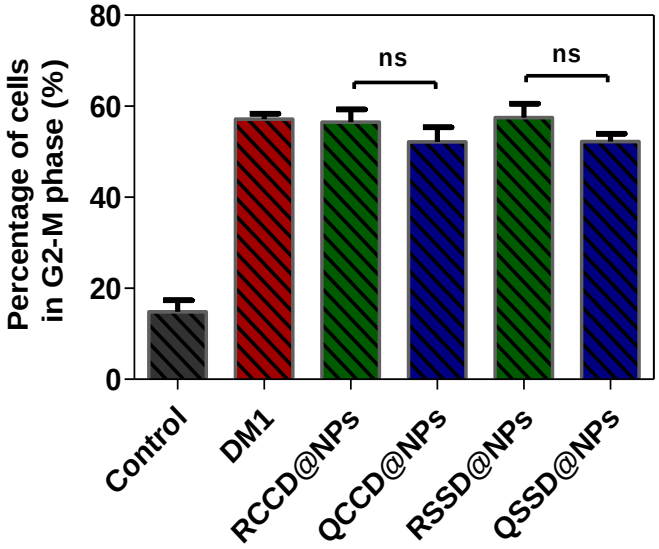

Figure S27. The percentage of cells in G2-M phase with different treatments of APDC@NPs at a drug dose of 50 nM (calculated by free DM1) for 12 h on MCF-7 cells (n=3). *$p < 0.05$, **$p < 0.01$, p = ns versus the passive cRPQfK groups.

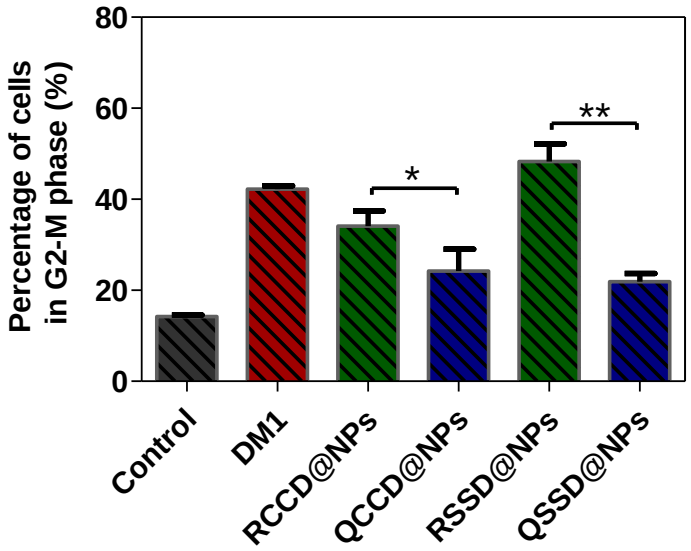

Figure S28. The percentage of cells in G2-M phase with different treatments of APDC@NPs at a drug dose of 50 nM (calculated by free DM1) for 12 h on HUVEC cells (n=3). *p < 0.05, **p < 0.01, p = ns versus the passive cRPQfK groups.

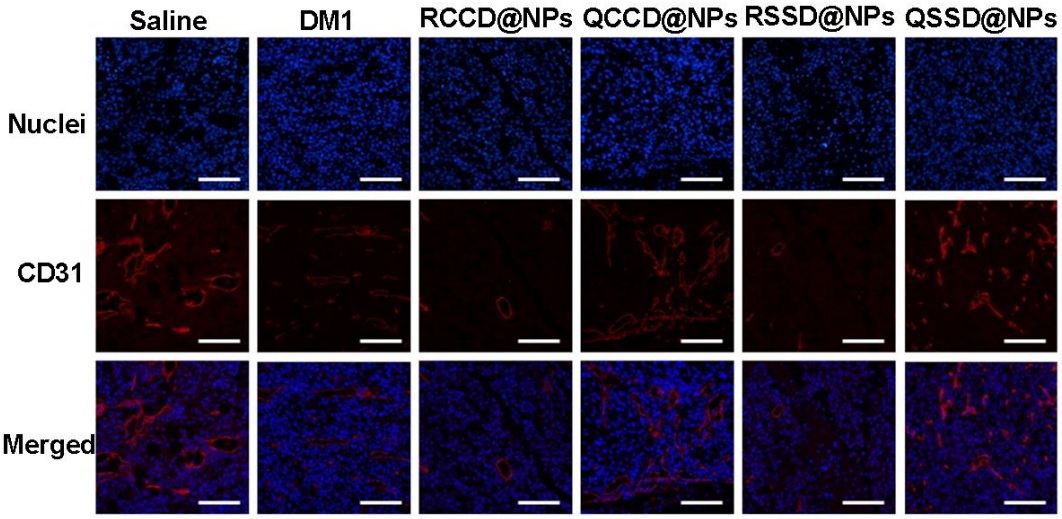

Figure S29. Confocal images of immunostaining with anti-CD31 for detecting tumor angiogenesis in tumor tissue after treatment of B16 tumor-bearing C57BL/6 mice with various APDC@NPs. Red represents the expression of CD31 on a tumor angiogenesis and blue represents nuclei stained by Hoechst 33258.

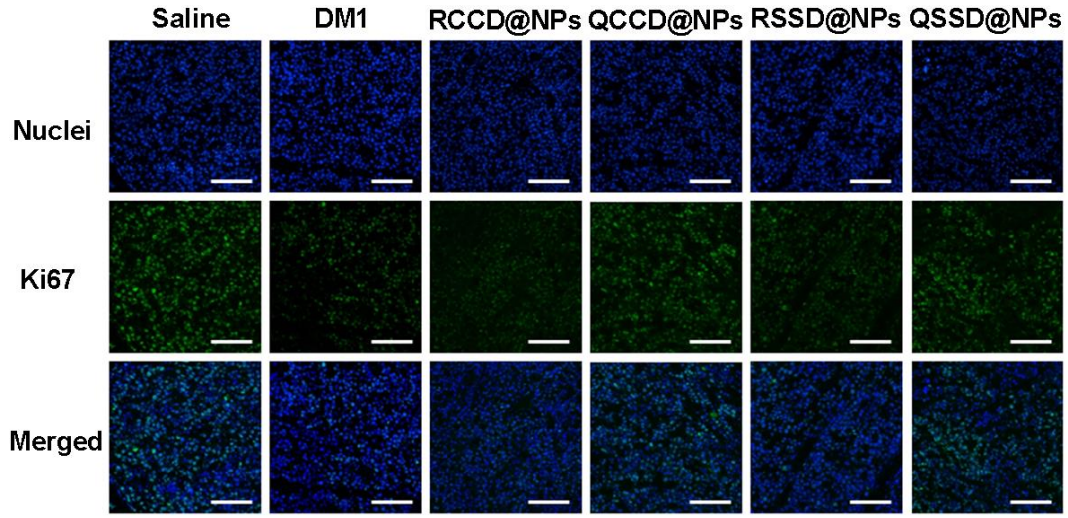

Figure S30. Fluorescent images of proliferating cells in tumor sections from different treatment groups. Tumor sections were immunostained with anti-Ki-67 nuclear antigen for cell proliferation. Green represents the expression of Ki67 on proliferating cells and blue represents nuclei stained by Hoechst 33258.